VIBRATION-DRIVEN ROBOTS WITH MOVABLE INTERNAL MASSES

Sergey Jatsun
Mechatronical Department
Kursk State Technical University
Russia
jatsun@kursknet.ru

Lupehina Irina
Mechatronical Department
Kursk State Technical University
Kursk, Russia

Andrey Yatsun
Mechatronical Department
Kursk State Technical University
Russia
ayatsun@yandex.ru

Klaus Zimmerman
Mechanical Department
University of Ilmenu
Germany

Igor Zeydis
Mechanical Department
University of Ilmenu
Germany

Abstract
In this article dynamics of original mobile micro-robots are developed. Vibration-driven robots use ideas of moving as periodical motion by vibration of internal masses or shape changing. Such kind of robots is especially useful for medical applications designed for the motion through rather narrow channels and realization stop-start regimes of the robot body with small length of step.

Key words
Mobile robot, vibration, motion, internal mass, control system.

1 Introduction
Vibration-driven mobile robots can move in various environments without wheels, caterpillars or legs. The propulsion of the robot is provided due to vibration of internal masses inside the robot and the interaction of the robot's body with the environment. The robot can move without separation from the supporting surface (Fig. 1) or hop (Fig. 2). On these figures we use following indication:1- robot body; 2- environment of robot; 3- supporting surface, 4- trajectory; F_z ,F_x – forces appearing as a result of motion of internal masses; R_z ,R_x – interaction forces between robot body and supporting surface; V- velocity of robot body.

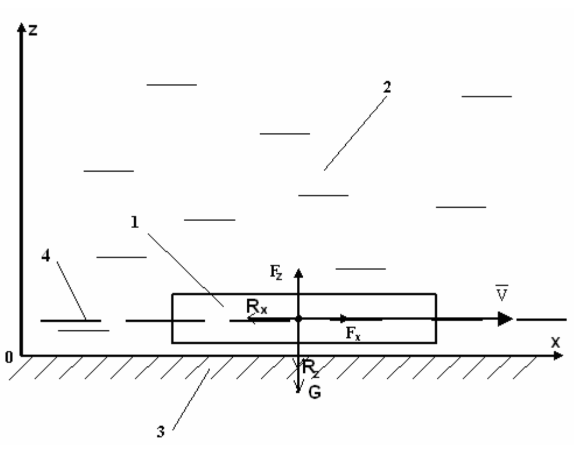

Figure 1. Motion of the vibration-driven robot without separation from the surface.

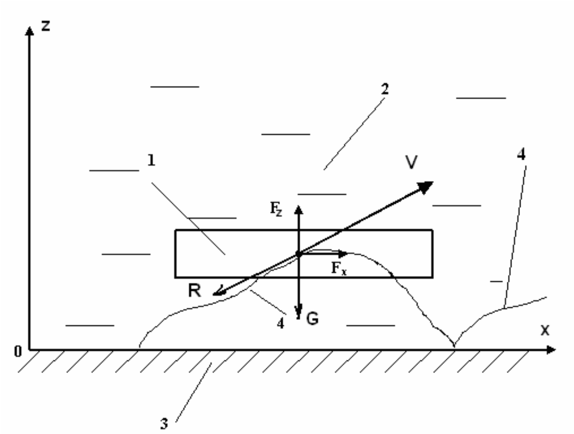

Figure 2. Hopping motion of the vibration-driven robot

Describing robots consist of a body with movable internal masses inside. The forces of interaction of the internal masses with the body and friction forces applied to the body by the environment enable the robot to move. Some aspects of the dynamics of motion of a body with an internal mass in a resisting medium and control of such a motion have been studied in different scientific papers. It has been indicated in that an asymmetry in the friction forces acting in the forward and backward directions is necessary for mobile vibration-driven robots. The most interesting idea for realization of high speed motion is idea of hopping robots.

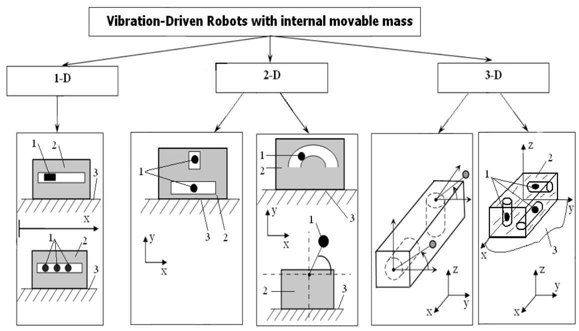

Figure 3. Classification of the Vibration –Driven Robots
1 – internal movable masses, 2 – robot body, 3 – supporting surface

This asymmetry of friction can be provided by anisotropy in the coefficient of friction (for example, due to a special coating of the contact surface), an asymmetry in the motion of the internal mass in the

horizontal direction or the asymmetry of the normal pressure due to the vertical motion of the internal mass.
Control of the direction and speed of the motion is provided by the regulation of the amplitude and the phase shift of the horizontal and vertical vibration excitation forces.

Classification of vibration – driven robots (see fig.3) is considered with point of view of dimensional of space where the robot and his parts moves.

In simplest case the robot moves in one-dimensional space or line (1-D). In this case displacement of the robot can be provided by motion of internal vibrating masses. In more complicate case the motion of robot is considered in two - dimensional space (2-D). This displacement may be realized with mobile internal masses moving with accordance of planar trajectory. The most complicated is motion of robot in three -dimensional (3-D) space. As it was in previous cases the motion of robot body can get by use of mobile internal masses that move in special tubes or rotate. In this paper we will consider 2-D robots.

2 Dynamic model of sliding robot.

The dynamical model of the vibration-driven robot with two internal masses, one of which moves in the horizontal direction and the other in the vertical direction, is schematically shown on fig. 4 [8, 9].

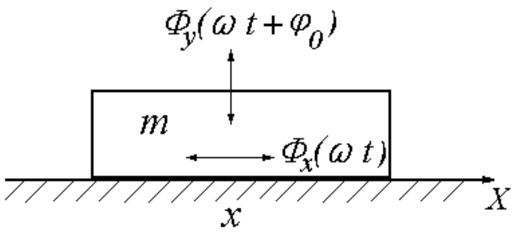

Figure 4. Dynamic model of the robot moving along a horizontal surface.

This model is represented by a body of mass m moving along a horizontal line OX under the action of the forces Φ_x and Φ_y caused by the motion of the internal masses relative to the robot's body and the environment resistance force (not shown in the figure). Mass m is equal to the total mass of the robot's body and the internal masses, $\Phi_x = -m_1\ddot{\xi}$, where m_1 and $\ddot{\xi}$ are the magnitude of the horizontally moving mass and the acceleration of this mass relative to the body, and $\Phi_y = m_2\ddot{\eta}$, where m_2 and $\ddot{\eta}$ are the magnitude and acceleration of the vertically moving mass.

We assume the excitation horizontal force Φ_x and Φ_y to be harmonic and shifted in phase by the angle φ_0 relative to one another,

$$\Phi_x = F_x \cdot \sin\omega t,\ \Phi_y = F_y \cdot \sin(\omega t+\varphi_0).$$

The supporting surface acts on the body with forces of dry friction, Φ_f, and viscous friction, Φ_v. The analytical expressions for these forces have the form:

$$\Phi_f = -\varepsilon \cdot f \cdot N \cdot \operatorname{sgn}\dot{x}, \quad \dot{x} \neq 0,$$

$$\Phi_v = -\varepsilon \cdot \mu \cdot \dot{x},$$

where f and μ are the coefficients of dry and viscous friction, respectively, N is the normal pressure force, and $\varepsilon << 1$.

The purpose of this paper is to establish basic qualitative features of the dynamic behavior of vibration-driven robots and to investigate the possibilities for the control of such robots. To reach this goal, it could be helpful to have analytical relations, even for simplified cases. To do this end, we assume the friction forces to be small value, which is reflected in the small parameter ε occurring in the expressions for these forces.

Taking into account the expression for the normal pressure force, one can express the dry friction force as follows:

$$\Phi_f = -\varepsilon \cdot f\left[mg + F_y \cdot \sin(\omega t+\varphi_0)\right]\operatorname{sgn}\dot{x} = -\varepsilon \cdot F(\dot{x},t),$$

if $\dot{x} \neq 0$.

On this stage we assume that $mg \geq F_y$ and that the robot does not separate from the surface. The equation of motion in this case has the form

$$m\ddot{x} - F_x \sin\omega t + \varepsilon\mu\dot{x} + \varepsilon F(\dot{x},t) = 0. \qquad (1)$$

Denote $\dot{x} = V$ and make the change of variables

$$u = V + \frac{F_x}{m\omega}\cos\omega t, \qquad (2)$$

to reduce Eq. (1) to a standard form:

$$\dot{u} = -\varepsilon\left[\frac{\mu}{m}\cdot\left(u - \frac{F_x}{m\omega}\cos\varphi\right) + \frac{1}{m}F\left(u - \frac{F_x}{m\omega}\cos\varphi, t\right)\right], \quad \varphi = \omega t \qquad (3)$$

3 Numerical simulations

The results of the numerical simulation of the motion of the robot are shown in Figs. 5 and 6. The simulation involved the solution of the differential equations (1) and (3) subjected to the initial conditions $x(0)=0$, $\dot{x}(0)=0$, and $u(0)=0$. The calculations were performed for $m=0.1$, $g=9.81$, $F_x=2$, $F_y=0.9$, $\omega=20$ and various values of the friction coefficients εf and $\varepsilon\mu$. Here and in what follows, all quantities are measured in SI units.

Figure 5 presents the time history of the velocity V obtained by solving numerically the exact equation of motion (Eq. (1)) with $\varepsilon f = 0.5$ and $\varepsilon\mu = 0.2$. Figure 2 corresponds to different values of the phase shift angle φ_0: $\varphi_0 = \pi/2$ for Fig. 2a and $\varphi_0 = 5\pi/6$ for Fig. 2b. Note that the maximum average velocity in this case is not attained at $\varphi_0 = \pi/2$, in contrast to the result of the asymptotic analysis. This disagreement is due to the fact that the friction coefficients $\varepsilon f = 0.5$ and $\varepsilon\mu = 0.2$ are not small enough and the asymptotic approximation has a noticeable error.

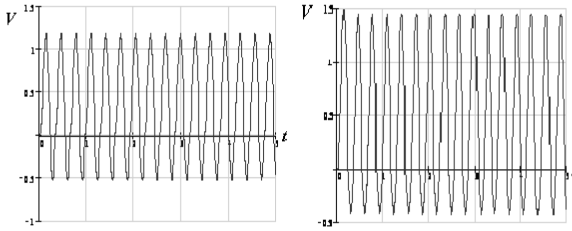
a) b)

Figure 5. Time history of the total velocity V at $\varepsilon f = 0.5$ and $\varepsilon\mu = 0.2$

a: $\varphi_0 = \pi / 2$, average velocity is 0.327;

b: $\varphi_0 = 5\pi / 6$, average velocity is 0.454

Figure 6 plots the average velocity of the robot $\langle V \rangle$ versus the phase shift angle φ_0 for various εf and $\varepsilon\mu$. Curves 1, 2, and 3 are correspond to ($\varepsilon f = 0.05$, $\varepsilon\mu = 0.02$), ($\varepsilon f = 0.05$, $\varepsilon\mu = 0.2$), and ($\varepsilon f = 0.05$, $\varepsilon\mu = 0.02$), respectively.

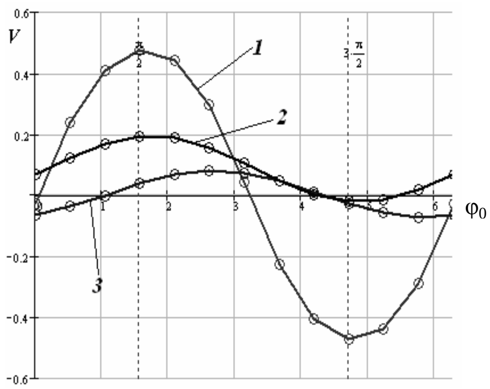

Figure 6. Average velocity of the robot versus the phase shift angle φ_0

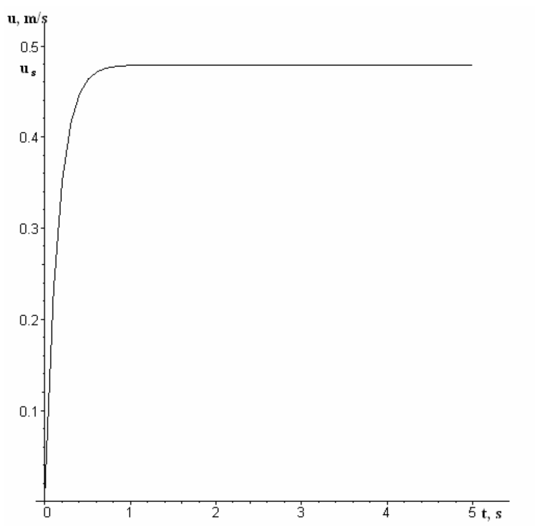

Figure 7. Time history of the slow component of the velocity u

Figure 7 shows the time history of the velocity of the average motion u obtained by solving numerically the averaged equation of (3) for $\varepsilon f = 0.5$ and $\varepsilon\mu = 0.2$. The value of the steady velocity u_s obtained by solving the transcendental equation is $u_s = 0.48$ m/s

Robots equipped with two-coordinate vibration exciters can move even in the absence of an asymmetry in the friction or vibration characteristics. The reverse in the direction of motion is provided by changing the phase difference between the vertical and horizontal excitation vibrations.

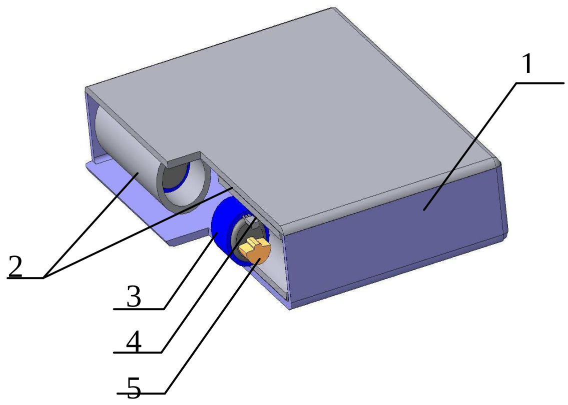

Figure 8. Scheme of sliding robot with internal rotating mass (angle φ_0 equal 90^0).

Fig.8 shows the scheme of sliding robot with two internal rotating masses. In this case angle φ_0 equal 90^0. Prototype of robot consists of robot body 1; electromotor frames 2; electro motors 3; encoder 4 and rotating masses 5.

4 Hopping vibration – driven robot

On this stage we assume how the robot can separate from the supporting surface. If shows previous analysis robot body has maximum velocity for angle φ_0 equal 90^0. Therefore we will consider hopping robot for this case. It means that internal mass is rotating around central point of robot body. Calculating scheme of the hopping robot on the fig.9 is shown.

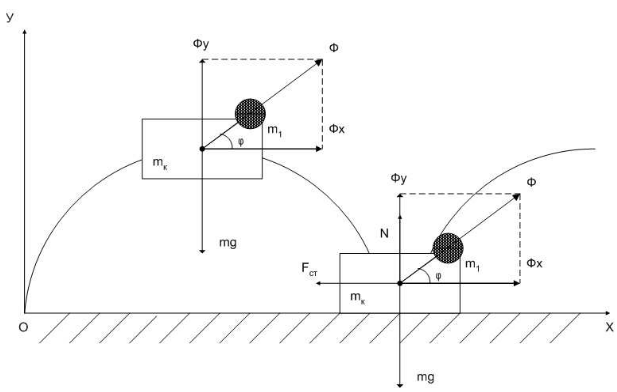

Figure 9. Calculating scheme of the hopping robot

5 Mathematical model of hopping robot

The motion of vibrating driven hopping robot can be described by system of differential equations. In a case when $y>0$, pressure force of supporting surface equal zero $(N=0)$ and motion can be described by following equations:

$$\begin{cases} m\ddot{x} = \Phi_x, \\ m\ddot{y} = \Phi_y - mg, \end{cases} \qquad (4)$$

where m – full mass of vibration - driven robot;

$$m = m_1 + m_\kappa,$$

m_1 –mass of rotating body;
m_κ –mass of robot body.

Force Φ, acting on the robot body, is determined as

$$\Phi = m_1\omega^2 r, \qquad (5)$$

where ω – frequency of rotation of internal moss;
r – distance between centers of masses;
Projections of force Φ can be defined in a next form:

$$\begin{cases} \Phi_x = \Phi \cdot \cos\varphi, \\ \Phi_y = \Phi \cdot \sin\varphi, \end{cases} \qquad (6)$$

φ – angle between vector Φ and axis Ox.
Angle φ is function of the time

$$\varphi = \omega t + \psi, \qquad (7)$$

ψ –shift phase angle, defining by initial position of internal rotating mass.

In simplest case, each step begins with such conditions:

$$1.\ \dot{x} \neq 0,\ \dot{y} \neq 0$$

$$2.\ \dot{x} \neq 0,\ \dot{y} = 0$$

$$3.\ \dot{x} = 0,\ \dot{y} = 0$$

When $y=0$, the motion of considering system describing by differential equations:

$$\begin{cases} m\ddot{x} = \Phi_x + F_{TP}, \\ N = mg - \Phi_y, \end{cases} \qquad (7)$$

Where F_{TP} – dry friction force:

$$F_{TP} = \begin{cases} -fN\mathrm{sign}(\dot{x}_2), & \text{if } \dot{x} \neq 0, \\ -F_0, & \text{if } \dot{x} = 0 \text{ and } |F_0| \leq fN, \\ -fN\mathrm{sign}(F_0), & \text{if } \dot{x} = 0 \text{ and } |F_0| > fN \end{cases} \qquad (8)$$

f –friction coefficient; N-normal pressure force, F_0 – summ of external forces.

The results of numerical solution of equations (4) and (8) are introduced on the figures in a form of time history of coordinates x and y and trajectories of central point of robot body. For solution of these equations special calculating algorithm was developed. Analysis of the results shows the shape of the trajectory of hopping motion depended on frequency and relation m_1r/m. Figures 13-15 illustrate completely different trajectories of robot body. Fig.16 introduce diagram of regimes of hopping motion of robot body. It is defined at least three zones providing the hopping motion. Zone 1 corresponds to trajectory introduced on diagram fig.12. Zone 2 accordingly - trajectory introduced on diagram fig.13. Zone 3 - trajectory introduced on diagram fig.14.

.

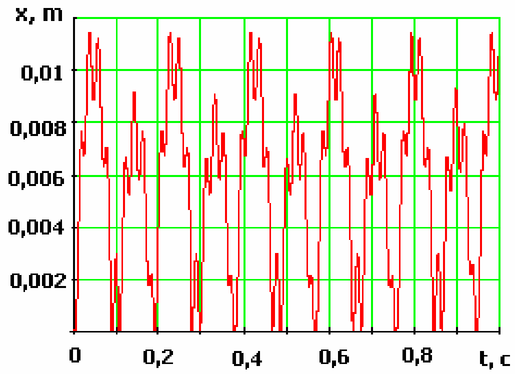

Figure 10. Time history of the coordinate y (frequency 210 1/s).

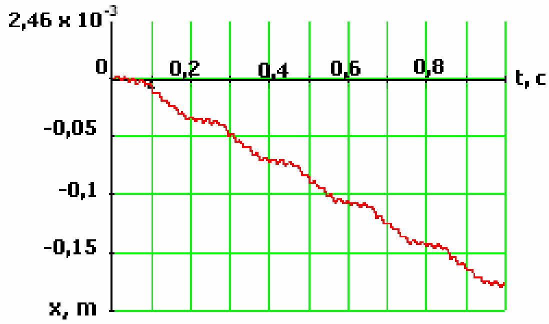

Figure 11. Time history of the coordinate x (frequency 210 1/s).

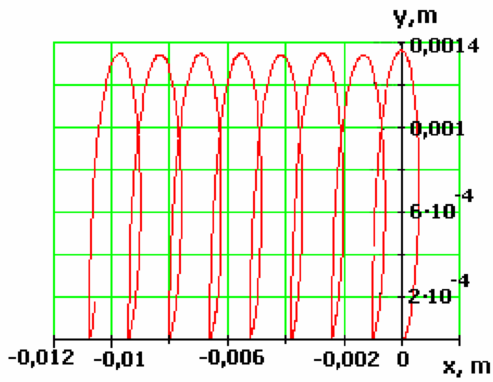

Figure 12. Trajectory of central point of robot body for one revolution of internal mass while one hop.

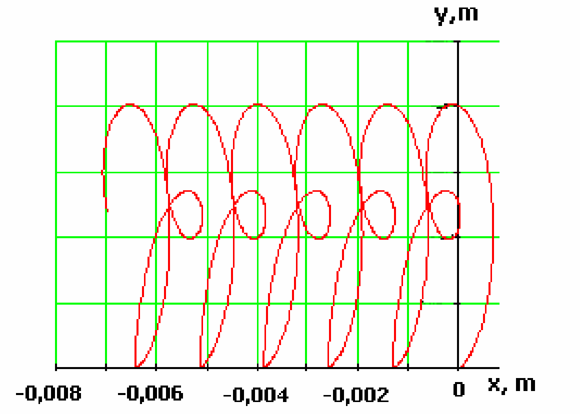

Figure 13. Trajectory of central point of robot body for two revolutions of internal mass while one hop.

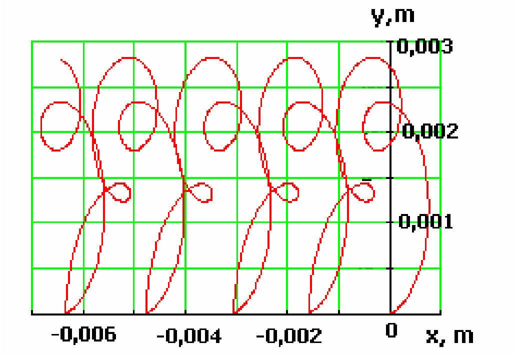

Figure 14. Trajectory of central point of robot body for three revolutions of internal mass while one hop.

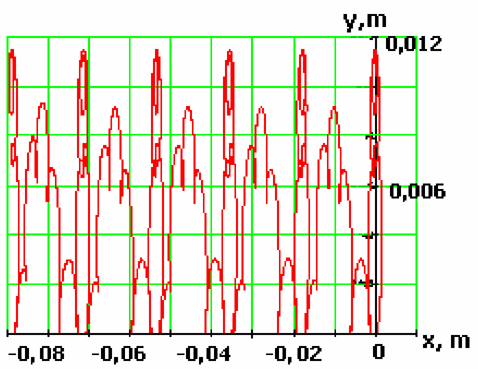

Figure 15. Trajectory of central point of robot body for fore revolutions of internal mass while one hop.

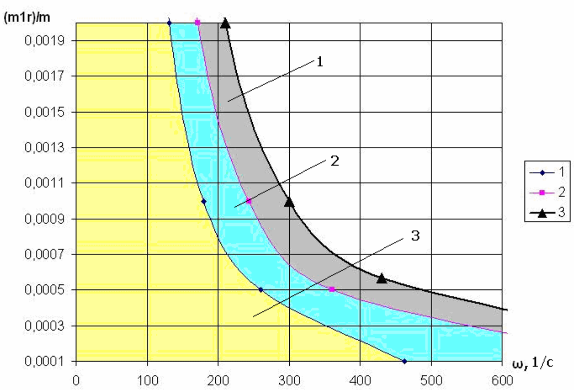

Figure 16. Diagram of different regimes of hopping of robot body dependence on frequency and relation m_1 r/m.

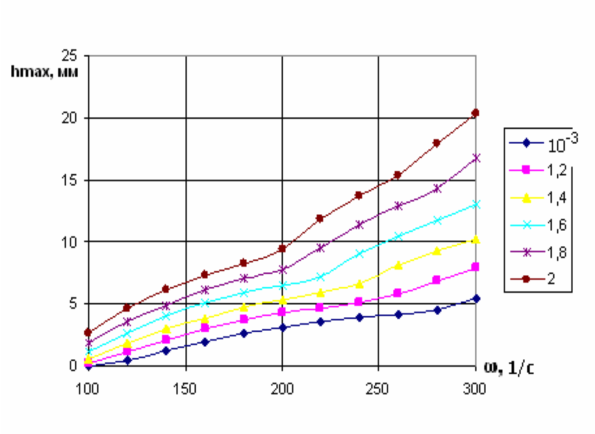

Figure 17. Diagram of maximal height of hopping robot dependence on frequency and parameter m_1 r/m.

Diagram on fig.17 shows dependence on maximal height of hopping robot dependence on frequency. We defined that height of hopping robot increase when frequency goes up. It is interesting that maximum average velocity corresponds to frequency equal about 260 1/s (see fig. 18).

It is very important to reduce the vibration level transmitted to the equipment of the robot from the exciters it is reasonable to place this equipment on a special platform, isolated from the vibration-driven robot body by a spring-dashpot vibration absorber. We have considered viscous - elasticity supporting element. Parameters of this element are calculated by assistance of finite element method in SolidWorks software. Result of deformation calculation is shown on fig. 19. Fig. 20 shows the scheme of prototype of hopping robot with rotating masses. The robot consists of five main part two DC –motors maintained in a frame, IR-sensors, vibration absorber and control system.

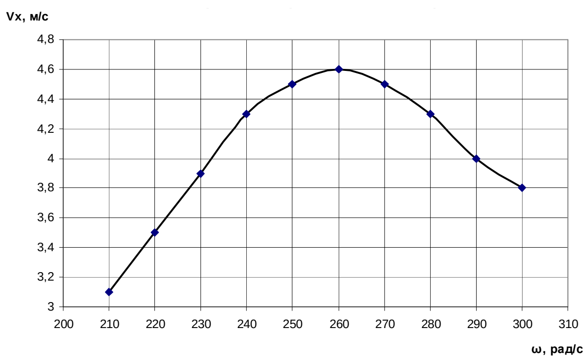

Figure 18. Diagram of average velocity of robot body dependence on frequency for $(m1 \cdot r)/m = 2{,}34 \cdot 10^{-4}$.

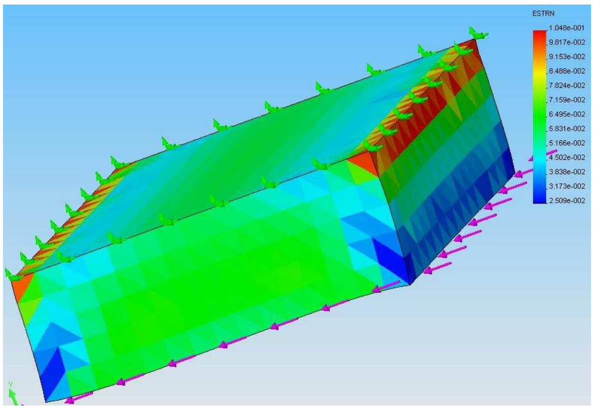

Figure 19. Calculation of deformation of viscous - elasticity element by FEM method.

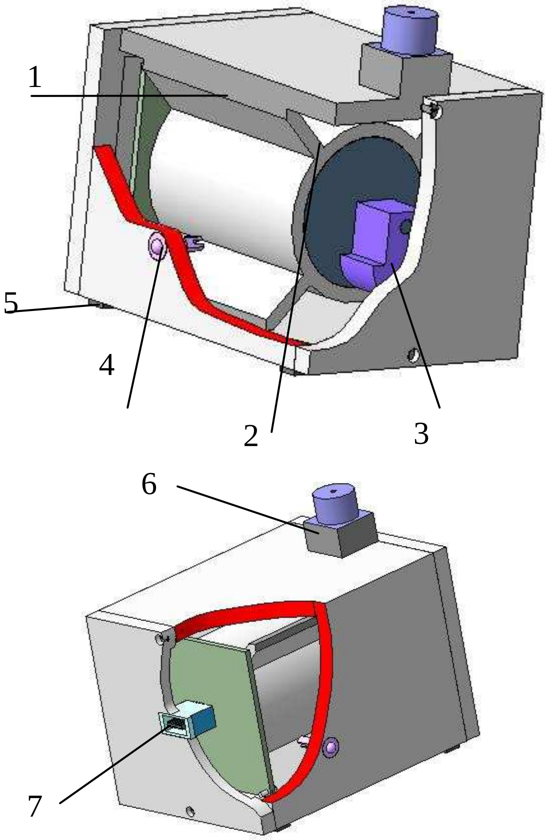

Figure 20. The scheme of prototype of hopping robot with rotating masses.
1 –robot body, 2 –frame of electrical DC-motor, 3 –rotating internal mass, 4 –IR – sensor , 5 – Viscous - elasticity elements, 6 – video camera, 7-USB – connector.

We have simulated landing process of the robot body for different parameters of viscous - elasticity elements. Some results on the fig. 21 are shown. This diagram introduces acceleration 1 and displacement of robot body 2 dependence on time. Our investigation has shown that level of acceleration can be decreased in many times comparing with landing of rigid body.

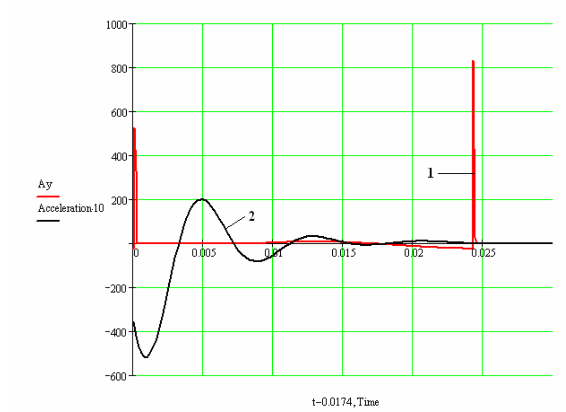

Fig.21. Diagram of impact acceleration and displacement of robot body during landing on the supporting surface

6. Conclusions

In this paper original schemes of mobile robots for sliding and hoping motion with rotating internal masses, were developed. Mathematical models of 1-D and 2-D vibration-driven robots were presented. By analytical method average velocity of robot body in different motion regimes were calculated. Numerical algorithm for calculation of dynamical parameters of motion allowed investigating periodical regimes of motion.

Acknowledgment

This investigation is supported by RBRF project №04-01-04002, №05-08-33382.

References

Aoshima, S.; Tsujimura, T.; Yabuta, T.: A miniature mobile robot using piezo vibration for mobility in a thin tube. Journal of Dynamic Systems, Measurement, and Control Vol. 115 (1993), pp. 270-278

Yeh, R.; Hollar, S.; Pister, K.S.J.: Design of low-power silicon articulated microrobots. Journal of Micromechatronics, Vol. 1, Num. 3, 2001, pp. 191-203

Gradetsky, V.G.; Knyazkov, M.M.; Kravchuk, L.N.; Solovtsov, V.N.: Microsensor control of motion of compact robots inside tubes (in Russian), Mikrosistemnaya Tekhnika [Microsystem Engineering], No. 8, 2002, pp. 11–19

Ma, J.; Lo, M.; Bao, Z.; Wang, A.: Micro peristaltic robot simulating earthworm and its control system. Journal of Shanghai Jiaotong University Vol. 33 No. 7, 1999

Bolotnik N.N., Chernousko F.L., Kostin G.V., and Pfeiffer F. Regular motion of a tube-crawling robot in a curved tube // Mechanics of Structures and Machines. 2002. Vol. 30. No. 4. P. 431-462.

Panagiotis Vartholomeos, Evagelos Papadopolos. Dynamics, Design and Simulation of Novel Microrobotic Platform Employing Vibration Microactuators. Journal of Dynamics System, Measurement and Control. Vol.128, March 2006 pp.122-133.

Bolotnik N.N., Zeidis I.M., Zimmermann K. and Yatsun S.F. Dynamics of Controlled Motion of Vibration-Driven systems. Journal of Computer and Systems Science International,2006 Vol45 № 5pp.834-840.

Bolotnik N.N., Zeidis I.M., Zimmermann K. and Yatsun S.F Mobile vibrating robots. Proceedings of the 9 th International Conference on climbing and welkin robots(CLAWAR2006). Brussels, Belgium. 2006. p.558-563.

Bolotnik N.N., Yatsun S.F., Chrepanov A.A. Automatically controlled vibration-driven. Proc. Intern conf. on mechatronics ICM2006. Budapest, 2006. p.438-441

Samuel Kesner, Jean – Sebastien Plante, Steven Dubovsky A Hopping mobility concept for a rough terrain search and rescue robot. Advances in climbing and walking robots.